Magnetotransport in conducting composite films with a disordered columnar microstructure and an in-plane magnetic field

David J. Bergman and Yakov M. Strelniker

School of Physics and Astronomy, Raymond and Beverly Sackler Faculty of Exact Sciences, Tel Aviv University, Tel Aviv 69978, Israel
(Received 26 May 1999)

Some exact relations are found between different elements of the bulk effective resistivity tensor of a two-component composite medium with a columnar microstructure. A self-consistent effective-medium approximation is constructed that incorporates those relations. This is then used to conduct a theoretical study of magnetotransport in such a medium, which can be implemented experimentally as a thin conducting film with perpendicular cylindrical inclusions. Detailed, explicit results are obtained for a conductor/insulator random mixture and a normal conductor/perfect conductor random mixture that are above the two-dimensional percolation threshold of the normal conducting constituent. At large magnetic fields $\mathbf{B}$, the in-plane magnetoresistance components increase as $\mathbf{B}^2$ *without any saturation* in mixtures of the first kind, but tend to constant asymptotic values in mixtures of the second kind. The Clausius-Mossotti or Maxwell Garnett type of approximation, which predicts a different behavior, is shown to be unreliable at strong magnetic fields even for very dilute mixtures. [S0163-1829(99)06641-2]

I. INTRODUCTION

Following the early pioneering work of many years ago by Landauer and his associates,[1] it has become apparent, over the last 15 years, that among the various physical properties of macroscopically inhomogeneous or composite media, magnetotransport exhibits unique forms of behavior. This is due to the fact that the material response, although linear, is characterized by a *nonsymmetric (electrical conductivity) tensor*, and to the fact that this tensor has a *nonlinear dependence* on the magnetic field $\mathbf{B}$.[2-13] Some of those developments are described in a 1992 review article on physical properties of macroscopically inhomogeneous media.[14] More recently, composite structures with a columnar microstructure, i.e., a structure that is uniform along a columnar symmetry axis, have received some attention. It was found that periodic structures of this kind, e.g., a two-dimensional array of parallel cylindrical holes in an otherwise uniform conducting medium, exhibit a very strong and very anisotropic magnetoresistance when $\mathbf{B}$ is strong and is perpendicular to the cylinder axes, i.e., both the longitudinal bulk effective resistivity component $\rho_\parallel^{(e)}$ and the in-plane transverse bulk effective resistivity component $\tilde{\rho}_\perp^{(e)}$ were found to oscillate strongly when $\mathbf{B}$ was rotated in the perpendicular plane.[15] Very recently, this behavior was shown to arise due to local currents that flow along the cylinder axes. Such currents, when present, continue to increase without any limit as $\mathbf{B}$ increases, leading to a positive magnetoresistance that never saturates when $\mathbf{B}$ and the volume averaged current density $\langle \mathbf{J} \rangle$ point in certain in-plane directions.[16-19]

Here we discuss the case of a disordered columnar microstructure. In that case we do not expect any dependence of $\rho_\parallel^{(e)}$ or $\tilde{\rho}_\perp^{(e)}$ on the direction of $\mathbf{B}$. But we do expect those resistivities to exhibit a nonsaturating dependence on $\mathbf{B}$, due to the nonsaturating local currents along the columnar axis, as mentioned before. We also expect to find critical behavior when such a system is near a two-dimensional percolation

threshold. In order to study such systems, we develop a self-consistent effective-medium approximation that is a variant of the well-known approximation invented by Bruggeman many years ago.[20] Generalizations of that approximation were developed previously for application to magnetotransport.[21-24] However, for the columnar systems under discussion here it appears that those generalizations violate some exact relations that must hold between the various elements of the bulk effective resistivity tensor $\hat{\rho}_e$. We discovered those relations recently, and they are presented here. Our variant of the self-consistent effective medium approximation takes into account those exact relations, and enables us to set up a system of coupled algebraic equations for $\rho_\parallel^{(e)}$ and $\tilde{\rho}_\perp^{(e)}$ in the case of a two-component composite where both constituents are isotropic conductors. We exploit this approximation in order to discuss the case of a conductor/insulator mixture, and the case of a normal conductor/perfect conductor mixture.

The rest of this article is organized as follows: In Sec. II we derive the exact relations which $\hat{\rho}_e$ must satisfy in a two-component columnar composite. In Sec. III a self-consistent effective-medium approximation is developed that satisfies those relations. In Sec. IV that approximation is applied to the study of random columnar mixtures of conductor/insulator and of normal conductor/perfect conductor constituents. Section V provides a summary and discussion of the results obtained, and indicates directions for further work. In the Appendix we describe a method for finding the uniform electric field that appears inside an isolated conducting inclusion of ellipsoidal shape, which is embedded in an otherwise homogeneous conducting host, when a uniform electric field is applied at large distances. This is applied to the case of an inclusion shaped as a circular cylinder, which is an isotropic conductor, and a host, whose response can be anisotropic, but one of the principal axes of its resistivity tensor coincides with the cylinder axis. A uniform magnetic field is applied along another principal axis, so that both
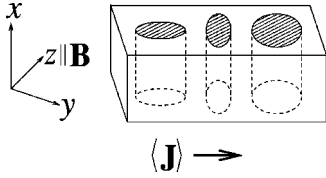
FIG. 1. Composite conductor with columnar microstructure shaped as a wire or thin film, with the film plane, magnetic field $\mathbf{B} \| z$, and volume-averaged current density $\langle \mathbf{J} \rangle$ all perpendicular to the columnar axis x.

resistivity tensors are nonsymmetric—this is needed in order to carry out the studies described in Sec. IV.

II. EXACT RESULTS FOR COLUMNAR SYSTEMS

Consider an infinite, three-dimensional conducting medium with columnar symmetry, i.e., the local resistivity and conductivity tensors $\hat{\rho}$ and $\hat{\sigma} = 1/\hat{\rho}$ depend only on the two Cartesian coordinates y and z, and are independent of x (see Fig. 1). When boundary conditions are applied, which would result in uniform values for the local electric field $\mathbf{E}$ and local current density $\mathbf{J}$ if the system were homogeneous, then the actual local values of those quantities *in the inhomogeneous system* will also depend only upon y and z. Moreover, it is easily shown that the requirement $\nabla \times \mathbf{E} = 0$ then leads to the result that E_x, the component of $\mathbf{E}$ along the columnar symmetry axis, is *uniform everywhere*. These results are valid regardless of the detailed form of $\hat{\rho}$.[16] In particular, they continue to hold in the presence of a static magnetic field, when $\hat{\rho}$ and $\hat{\sigma}$ are nonsymmetric tensors.

We now turn to consider the bulk effective resistivity tensor $\hat{\rho}_e$ and conductivity tensor $\hat{\sigma}_e = 1/\hat{\rho}_e$, which are defined so as to characterize the linear relation between the volume averaged fields $\langle \mathbf{E} \rangle$, $\langle \mathbf{J} \rangle$:

$$\langle \mathbf{E} \rangle \equiv \hat{\rho}_e \cdot \langle \mathbf{J} \rangle. \tag{2.1}$$

We now show that some exact relations must exist among the elements of $\hat{\rho}_e$ in the case of a two-component composite medium with a columnar microstructure—these are a consequence of the uniformity of E_x. We use the notation $\langle \; \rangle_1$, $\langle \; \rangle_2$ to denote averages over the subvolumes of the two constituents, and p_1, $p_2 = 1 - p_1$ to denote the two volume fractions, and $\hat{\rho}_1$, $\hat{\rho}_2$ to denote the two resistivity tensors. It is clear that we have

$$\langle \mathbf{E} \rangle = p_1 \langle \mathbf{E} \rangle_1 + p_2 \langle \mathbf{E} \rangle_2, \quad \langle \mathbf{J} \rangle = p_1 \langle \mathbf{J} \rangle_1 + p_2 \langle \mathbf{J} \rangle_2, \tag{2.2}$$

and that from these relations and Eq. (2.1) we can obtain a linear relation between $\langle \mathbf{J} \rangle$ and $\langle \mathbf{J} \rangle_1$:

$$(\hat{\rho}_2 - \hat{\rho}_e) \cdot \langle \mathbf{J} \rangle = p_1 (\hat{\rho}_2 - \hat{\rho}_1) \cdot \langle \mathbf{J} \rangle_1. \tag{2.3}$$

These can be viewed as three equations that determine the three components of $\langle \mathbf{J} \rangle_1$, given the three components of $\langle \mathbf{J} \rangle$. Because $E_x = \langle E_x \rangle_1 = \langle E_x \rangle$ is uniform everywhere, we will get the same result when we average the *local relation*

$E_x = (\hat{\rho} \cdot \mathbf{J})_x$ either over the total volume, or just over the subvolume of a single constituent. This leads to another relation between $\langle \mathbf{J} \rangle$ and $\langle \mathbf{J} \rangle_1$:

$$(\hat{\rho}_e \cdot \langle \mathbf{J} \rangle)_x = (\hat{\rho}_1 \cdot \langle \mathbf{J} \rangle_1)_x. \tag{2.4}$$

Having to satisfy this equation, which is independent of the three previous equations (2.3), means that we have an overdetermined set of equations for the three components of $\langle \mathbf{J} \rangle_1$. Actually, there will be several sets of overdetermined equations for $\langle \mathbf{J} \rangle_1$, since one can make three independent choices for $\langle \mathbf{J} \rangle$. For example, we can single out each one of the average current components $\langle J_x \rangle$, $\langle J_y \rangle$, $\langle J_z \rangle$ to be nonzero, leading to three different sets of over-determined equations. Each of these sets will usually require some determinant to vanish in order to allow a consistent solution, and that will result in an exact relation among the elements of $\hat{\rho}_e$.

We now apply these general considerations to a particular case, where both constituents exhibit isotropic electrical response, and where a static magnetic field $\mathbf{B}$ is applied along the z axis. In that case, the constituent resistivity tensors have the form

$$\hat{\rho}_j = \begin{pmatrix} \rho_\perp^{(j)} & -\rho_H^{(j)} & 0 \\ \rho_H^{(j)} & \rho_\perp^{(j)} & 0 \\ 0 & 0 & \rho_\|^{(j)} \end{pmatrix}, \quad j = 1, 2. \tag{2.5}$$

If the z axis, which is perpendicular to the columnar symmetry axis x, is also a symmetry axis of the two-dimensional microstructure, then $\hat{\rho}_e$ also has a relatively simple form, namely,

$$\hat{\rho}_e = \begin{pmatrix} \rho_{xx}^{(e)} & -\rho_H^{(e)} & 0 \\ \rho_H^{(e)} & \rho_{yy}^{(e)} & 0 \\ 0 & 0 & \rho_\|^{(e)} \end{pmatrix}. \tag{2.6}$$

We note that, in general, we will have $\rho_{xx}^{(e)} \neq \rho_{yy}^{(e)}$, because the microstructure is definitely noninvariant with respect to *arbitrary three-dimensional rotations*. On the other hand, if the microstructure is invariant under *certain two-dimensional rotations* around the columnar axis, then of course $\hat{\rho}_e$ will retain its form under such rotations, if we apply the same rotations also to the magnetic field $\mathbf{B}$.

For such a system, the z component of Eq. (2.3) decouples from the other equations and leads to no restriction on any elements of $\hat{\rho}_e$:

$$p_1 (\rho_\|^{(2)} - \rho_\|^{(1)}) \langle J_z \rangle_1 = (\rho_\|^{(2)} - \rho_\|^{(e)}) \langle J_z \rangle. \tag{2.7}$$

The x and y components of Eq. (2.3), as well as Eq. (2.4), then become a set of three equations for $\langle J_x \rangle_1$ and $\langle J_y \rangle_1$, given $\langle J_x \rangle$ and $\langle J_y \rangle$. By alternately choosing $\langle J_x \rangle = 0$ and $\langle J_y \rangle = 0$, we get two independent sets of over-determined equations for $\langle J_x \rangle_1$ and $\langle J_y \rangle_1$. Setting the two determinants equal to 0 leads, after some algebra, to the following exact relations among $\rho_{xx}^{(e)}$, $\rho_{yy}^{(e)}$, and $\rho_H^{(e)}$:

$$\rho_{xx}^{(e)}[(\rho_\perp^{(2)}-\rho_\perp^{(1)})(p_1\rho_\perp^{(2)}+p_2\rho_\perp^{(1)})+(\rho_H^{(2)}-\rho_H^{(1)})$$
$$\times(p_1\rho_H^{(2)}+p_2\rho_H^{(1)})]-\rho_H^{(e)}(\rho_\perp^{(2)}\rho_H^{(1)}-\rho_\perp^{(1)}\rho_H^{(2)})$$
$$=\rho_\perp^{(1)}(\rho_\perp^{(2)2}+\rho_H^{(2)2})-\rho_\perp^{(2)}(\rho_\perp^{(1)2}+\rho_H^{(1)2}), \qquad (2.8)$$

$$\rho_H^{(e)}[(\rho_\perp^{(2)}-\rho_\perp^{(1)})(p_1\rho_\perp^{(2)}+p_2\rho_\perp^{(1)})+(\rho_H^{(2)}-\rho_H^{(1)})$$
$$\times(p_1\rho_H^{(2)}+p_2\rho_H^{(1)})]+\rho_{yy}^{(e)}(\rho_\perp^{(2)}\rho_H^{(1)}-\rho_\perp^{(1)}\rho_H^{(2)})$$
$$=\rho_H^{(1)}(\rho_\perp^{(2)2}+\rho_H^{(2)2})-\rho_H^{(2)}(\rho_\perp^{(1)2}+\rho_H^{(1)2}). \qquad (2.9)$$

These relations become especially simple in the important limiting case $\hat\rho_2\gg\hat\rho_1$. In that case, Eq. (2.9) leads to

$$p_1\rho_H^{(e)}\cong\rho_H^{(1)}-\rho_{yy}^{(e)}\frac{\rho_\perp^{(2)}\rho_H^{(1)}-\rho_\perp^{(1)}\rho_H^{(2)}}{\rho_\perp^{(2)2}+\rho_H^{(2)2}}. \qquad (2.10)$$

The second term on the right-hand side (rhs) is only important if $\rho_{yy}^{(e)}=O(\hat\rho_2)$, namely, if constituent 2 percolates in the y,z plane. If that is not the case, which means that constituent 1 does percolate in that plane, then Eq. (2.10) reduces to the simple result,

$$\rho_H^{(e)}=\frac{\rho_H^{(1)}}{p_1} \text{ for } \hat\rho_2=\infty \text{ and } \hat\rho_1 \text{ percolating in plane.} \qquad (2.11)$$

Under the same condition $\hat\rho_2\gg\hat\rho_1$, Eq. (2.8) leads to the equally simple result,

$$\rho_{xx}^{(e)}=\frac{\rho_\perp^{(1)}}{p_1} \text{ for } \hat\rho_2=\infty. \qquad (2.12)$$

In the following section, these exact relations will be used to develop a self-consistent effective-medium approximation that differs from the conventional generalization of Bruggeman's self-consistent effective-medium approximation to anisotropic conductivity, as developed, for example, in Ref. 23.

III. SELF-CONSISTENT EFFECTIVE-MEDIUM APPROXIMATION

A. General remarks

Most approximations of this type are extensions or generalizations of the original self-consistent effective-medium approximation, which was formulated many years ago by Bruggeman[20] and by Landauer.[25] Those extensions have included anisotropic constituents[23] and columnar microstructures[24] in the presence of a magnetic field. Another extension of the basic idea that underlies these approximations leads to the well-known coherent potential approximation, used extensively in quantum-mechanical treatments of disordered systems.[26–28]

One way to derive the Bruggeman-type approximations is to seek a homogeneous ''effective medium'' by the following procedure: The total change in bulk effective conductivity is first calculated for the case where a single inclusion of volume V_{inc} is embedded in a much larger volume V of the effective medium—the total change in conductivity will then be of order $V_{inc}/V\ll1$. The conductivity of the fictitious homogeneous effective medium is then determined by requiring that the total change in conductivity vanish when averaged over the different types of inclusions.[29] When the inclusions are shaped as ellipsoids, the change in conductivity can be calculated exactly to leading order in $V_{inc}/V\ll1$, therefore explicit equations are obtained for the conductivity of the effective medium. This approach, which reproduces all the usual self-consistent effective-medium results, has some advantages compared to other approaches.

(i) One avoids having to decide which average to use, because the change in total conductivity produced by a single inclusion is very small. Thus, to order $V_{inc}/V\ll1$, all averages are equivalent to the arithmetic average. Due to this circumstance, we find it appropriate to call this approach the ''unambiguous self-consistent effective-medium approximation[29] (USEMA).''

(ii) This approach can be extended also to nonlinear composites, where other approaches run into serious difficulties.[29–31]

A simple way to implement USEMA, in the case where the inclusions are assumed to have an ellipsoidal shape, is based on the fact that the internal electric field $\mathbf{E}_{int}$ in an isolated inclusion is uniform when a uniform external field $\mathbf{E}_0=\langle\mathbf{E}\rangle$ is applied at large distances. The relation between those fields is linear (see the Appendix)

$$\mathbf{E}_{int}=\hat\gamma_{inc}\cdot\mathbf{E}_0, \qquad (3.1)$$

and the matrix $\hat\gamma_{inc}(\hat\sigma_{inc},\hat\sigma_{host})$ depends on the conductivity tensors of the host and inclusion, as well as on the shape and orientation of the inclusion. When $\langle\mathbf{E}\rangle=\mathbf{E}_0$ is given, then the change in $\langle\mathbf{J}\rangle$ caused by a single inclusion is

$$\langle\mathbf{J}\rangle-\hat\sigma_{host}\cdot\mathbf{E}_0=\frac{V_{inc}}{V}(\hat\sigma_{inc}-\hat\sigma_{host})\cdot\mathbf{E}_{int}$$

$$=\frac{V_{inc}}{V}(\hat\sigma_{inc}-\hat\sigma_{host})\cdot\hat\gamma_{inc}\cdot\mathbf{E}_0, \qquad (3.2)$$

to leading order in V_{inc}/V.

This basic result can be used to derive the dilute approximation, in which the changes produced by different *isolated inclusions* are added together, ignoring any interactions. Using the fact that $\langle\mathbf{J}\rangle=\hat\sigma_e\cdot\mathbf{E}_0$, where $\hat\sigma_e\equiv1/\hat\rho_e$, this leads to the following simple equation for the bulk effective conductivity tensor in the dilute approximation $\hat\sigma_{e\,dil}$,

$$\hat\sigma_{e\,dil}-\hat\sigma_{host}=\langle(\hat\sigma_{inc}-\hat\sigma_{host})\cdot\hat\gamma_{inc}\rangle$$

$$=\sum_{j\neq host}p_j\langle(\hat\sigma_j-\hat\sigma_{host})\cdot\hat\gamma_{inc}(\hat\sigma_j,\hat\sigma_{host})\rangle_j. \qquad (3.3)$$

Here the sum is over the different types of inclusions j, *excluding the host component*, each with its particular volume fraction p_j, and $\langle\rangle_j$ signifies an average over the distribution of shapes and orientations of the inclusions of type j, including an average over the orientations of the principal axes of $\hat\sigma_j$. The Clausius-Mossotti– (or Maxwell Garnett–)type approximation (CMTA) for the bulk effective conductivity tensor, denoted by $\hat\sigma_{e\,CM}$, can be obtained by equating the average that appears in this equation to the result that would be

obtained by having a single inclusion of a particular shape, made of the effective medium *but occupying the entire volume*, i.e., with a volume fraction equal to 1:

$$(\hat{\sigma}_{e\,CM} - \hat{\sigma}_{host}) \cdot \hat{\gamma}_{inc}(\hat{\sigma}_{e\,CM}, \hat{\sigma}_{host})$$

$$= \sum_{j \neq host} p_j \langle (\hat{\sigma}_j - \hat{\sigma}_{host}) \cdot \hat{\gamma}_{inc}(\hat{\sigma}_j, \hat{\sigma}_{host}) \rangle_j. \qquad (3.4)$$

Finally, the unambiguous self-consistent effective-medium approximation, denoted simply by $\hat{\sigma}_e$, is obtained by taking the host to be the fictitious, uniform, effective medium, and requiring that the change in $\langle \mathbf{J} \rangle$ vanish when averaged over the different kinds of inclusions in that medium:

$$0 = \langle (\hat{\sigma}_{inc} - \hat{\sigma}_e) \cdot \hat{\gamma}_{inc}(\hat{\sigma}_{inc}, \hat{\sigma}_e) \rangle$$

$$= \sum_j p_j \langle (\hat{\sigma}_j - \hat{\sigma}_e) \cdot \hat{\gamma}_{inc}(\hat{\sigma}_j, \hat{\sigma}_e) \rangle_j. \qquad (3.5)$$

Here the sum is over *all* the different constituents j, each with its particular volume fraction p_j, and $\langle \rangle_j$ again signifies an average over the distribution of shapes and orientations of the constituent particles of type j, including an average over the orientations of the principal axes of $\hat{\sigma}_j$. This is equivalent to conventional extensions of the Bruggeman self-consistent effective-medium approximation (see Ref. 23).

If $\hat{\sigma}_{inc}$ and $\hat{\sigma}_{host}$ are both scalar tensors, and if we choose the coordinate axes to lie along the major axes of the ellipsoidal inclusion, then $\hat{\gamma}_{inc}$ is a diagonal matrix, whose nonzero elements are[32]

$$\gamma_{\alpha\alpha}(\sigma_{inc}, \sigma_{host}) = \frac{\sigma_{host}}{(1 - n_\alpha)\sigma_{host} + n_\alpha \sigma_{inc}}, \qquad (3.6)$$

where n_α is the depolarization factor along the major axis α. In general, however, the determination of $\hat{\gamma}_{inc}$ is nontrivial when $\hat{\sigma}_{inc}$ and $\hat{\sigma}_{host}$ are nonscalar tensors. A general method for doing this is presented in the Appendix. In the following subsection we apply that approach to the development of a self-consistent effective-medium approximation for columnar microstructures.

B. Columnar microstructures

For the columnar systems under consideration here, the straightforward implementation of USEMA, described in Sec. III A, leads to results that are consistent with earlier work.[24] However, when the constituent resistivities are nonscalar tensors, these results usually do not satisfy the exact relations that were obtained in Sec. II. Of course, we could impose those relations from the outset, thus there would be fewer unknowns among the matrix elements of $\hat{\rho}_e$. But the requirement of Eq. (3.5) would then lead to more equations than unknowns, and usually there would be no solution.

In order to overcome this dilemma, we must reduce the number of equations. In order to do this in a sensible fashion, we restrict our discussion to the case where a given value of $\langle \mathbf{J} \rangle$ is imposed upon the system. Moreover, we assume that, like $\mathbf{B}$, $\langle \mathbf{J} \rangle$ too is always perpendicular to the columnar axis (see Fig. 1). Those assumptions are natural ones to make

when the actual physical system is a thin film, in which a collection of perpendicular holes, or other inclusions, with constant (i.e., x independent) cross sections have been embedded. In experiments on such microstructures, the average of J_x always vanishes, while the constant field E_x is unmeasurable. We will therefore omit $\langle J_x \rangle$ and E_{0x} from the self-consistency requirements.

In order to do this, we first transform Eq. (3.2) into an expression for the change in $\langle \mathbf{E} \rangle \equiv \mathbf{E}_0$, caused by a single inclusion when $\langle \mathbf{J} \rangle$ is given:

$$\mathbf{E}_0 - \hat{\rho}_{host} \cdot \langle \mathbf{J} \rangle = \frac{V_{inc}}{V} (\hat{\rho}_{inc} - \hat{\rho}_{host}) \cdot \hat{\sigma}_{inc} \cdot \mathbf{E}_{int}$$

$$= \frac{V_{inc}}{V} (\hat{\rho}_{inc} - \hat{\rho}_{host}) \cdot \hat{\sigma}_{inc}$$

$$\cdot \hat{\gamma}_{inc}(\hat{\sigma}_{inc}, \hat{\sigma}_{host}) \cdot \hat{\rho}_{host} \cdot \langle \mathbf{J} \rangle. \qquad (3.7)$$

We then assume that $\langle J_x \rangle = 0$, and only require that the changes in E_{0y}, E_{0z} vanish when averaged over the different kinds of inclusions. This only involves the four elements yy, zz, yz, zy of the 3×3 matrix $(\hat{\rho}_{inc} - \hat{\rho}_{host}) \cdot \hat{\sigma}_{inc} \cdot \hat{\gamma}_{inc} \cdot \hat{\rho}_{host}$, which constitute the 2×2 submatrix in its lower right-hand corner. It is only this submatrix, which links between $\langle J_y \rangle$, $\langle J_z \rangle$ and E_{0y}, E_{0z} and is denoted by $[(\hat{\rho}_{inc} - \hat{\rho}_{host}) \cdot \hat{\sigma}_{inc} \cdot \hat{\gamma}_{inc} \cdot \hat{\rho}_{host}]_{\{yz\}}$, that must average out to 0 when $\hat{\rho}_{host} = \hat{\rho}_e$:

$$0 = \langle [(\hat{\rho}_{inc} - \hat{\rho}_e) \cdot \hat{\sigma}_{inc} \cdot \hat{\gamma}_{inc}(\hat{\sigma}_{inc}, \hat{\sigma}_e) \cdot \hat{\rho}_e]_{\{yz\}} \rangle$$

$$= \sum_j p_j \langle [(\hat{\rho}_j - \hat{\rho}_e) \cdot \hat{\sigma}_j \cdot \hat{\gamma}_{inc}(\hat{\sigma}_j, \hat{\sigma}_e) \cdot \hat{\rho}_e]_{\{yz\}} \rangle_j. \quad (3.8)$$

The average $\langle \rangle_j$ now denotes a two-dimensional average over shapes of columnar inclusions of type j, as well as a three-dimensional average over the orientation of the principal axes of the possibly anisotropic conductivity tensor $\hat{\sigma}_j$. The resulting approximation is called the ''columnar unambiguous self-consistent effective-medium approximation (CUSEMA).'' Clearly, Eq. (3.8) involves fewer self-consistency requirements than Eq. (3.5). There will also be a smaller number of unknowns whose values are determined by those equations, when the exact relations of Eqs. (2.8)–(2.12) are used. In general, the scalar equations for the elements of $\hat{\rho}_e$, which follow from the two approaches, will differ.

We note that, in the case of a columnar microstructure with isotropic constituents, where $\mathbf{B}$ is *parallel to the columnar axis* and an average $\langle \mathbf{E} \rangle$ or $\langle \mathbf{J} \rangle$ is prescribed in the perpendicular plane, all the local values of $\mathbf{E}$ and $\mathbf{J}$ also lie in that plane. This case has been studied before, both theoretically[1,24,33–35,3] and experimentally:[36] The physics becomes two-dimensional, and the behavior is very different from what is found when $\mathbf{B}$ lies in the perpendicular plane, which is the case under discussion here.

Finally, we note that the film should be not too thin if our present discussion is to be valid: As argued in the past, the film thickness l and the inclusion radius a must satisfy $a/l \ll \max(1, |\mu B|)$, where μ is the Hall mobility of the uniform film.[37]

IV. SOME PARTICULAR EXAMPLES OF COLUMNAR SYSTEMS

The matrix $\hat{\gamma}_{\mathrm{inc}}$ can be calculated in closed form for an inclusion that has the shape of an infinitely long circular cylinder. This is explained in the Appendix, where the explicit form of $\hat{\gamma}_{\mathrm{inc}}$ is calculated under the assumption that the inclusion is an isotropic conductor and the host, while anisotropic, has the principal axes of its conductivity tensor along the columnar axis x and the magnetic field $\mathbf{B}\|z$ [see Eqs. (A21)–(A24)]. The latter assumption is sufficiently general to allow for the anisotropy of $\hat{\rho}_e$ that is expected due to the columnar microstructure.

We now use these results in order to apply CUSEMA to a discussion of two interesting types of conducting columnar composite films, subject to an in-plane magnetic field: a conductor/insulator random mixture and a normal conductor/perfect conductor random mixture. In both of these systems we expect to find interesting behavior when $\mathbf{B}$ is large, and also when the normal conductor volume fraction p_M approaches the two-dimensional percolation threshold p_c from above.

In these systems, all types of inclusions are assumed to have isotropic electrical response, and are shaped as circular cylinders. Thus there is no need to average over the different types of orientations of the inclusions in Eq. (3.8). It is only necessary to calculate the 2×2 matrix $[(\hat{\rho}_{\mathrm{inc}}-\hat{\rho}_e)\cdot\hat{\sigma}_{\mathrm{inc}}\cdot\hat{\gamma}_{\mathrm{inc}}(\hat{\sigma}_{\mathrm{inc}},\hat{\sigma}_e)\cdot\hat{\rho}_e]_{\{yz\}}$ for the different inclusions. It is then a straightforward, though tedious, exercise to apply that equation. In particular, the off-diagonal elements of that matrix vanish identically. Also, the exact relations of Eqs. (2.8) and (2.9) reduce in these cases to simple results for $\rho_{xx}^{(e)}$ and $\rho_H^{(e)}$ [see Eqs. (2.10)–(2.12)]. Therefore we will finally have two coupled equations for the two unknowns $\rho_{yy}^{(e)}$ and $\rho_{zz}^{(e)}$. Because the xz, yz, zx, and zy elements of the matrices $\hat{\rho}_{\mathrm{inc}}$, $\hat{\rho}_e$, $\hat{\gamma}_{\mathrm{inc}}$ all vanish, therefore the scalar equation obtained in this way from the zz component of Eq. (3.8) is the same as the one obtained from the zz component of Eq. (3.5). By contrast, the equation obtained from the yy component of Eq. (3.8) includes contributions from the four different components xx, yy, xy, yx of Eq. (3.5), with coefficients that depend on those same components of $\hat{\rho}_e$. Therefore, the yy components of Eqs. (3.8) and (3.5) lead to two scalar self-consistency equations that are quite different.

For comparison, we will also calculate $\rho_{yy}^{(e)}$ and $\rho_{zz}^{(e)}$ using the CMTA of Eq. (3.4). We shall see that CUSEMA and CMTA usually predict very different behavior for these quantities at strong magnetic fields, even for very dilute mixtures. We will subsequently argue that CUSEMA is by far the more reliable of those approximations.

A. Disordered conductor/insulator mixture

We assume that the effective medium resistivity tensor $\hat{\rho}_e$ has the same form as $\hat{\rho}_{\mathrm{host}}$ of Eq. (A21), namely,

$$\hat{\rho}_e = \rho_M \begin{pmatrix} \alpha_e & -\beta_e & 0 \\ \beta_e & \gamma_e & 0 \\ 0 & 0 & \lambda_e \end{pmatrix}. \tag{4.1}$$

The resistivity tensor $\hat{\rho}_M$ of the conducting constituent is assumed to have the same form as $\hat{\rho}_{\mathrm{inc}}$ of Eq. (A22), namely,

$$\hat{\rho}_M = \rho_M \begin{pmatrix} 1 & -H_M & 0 \\ H_M & 1 & 0 \\ 0 & 0 & \nu_M \end{pmatrix}, \tag{4.2}$$

while that of the insulating constituent has the form $\hat{\rho}_I = \rho_I \hat{I}$, where $\hat{I}$ is the unit tensor. We assume that the M constituent percolates in the plane perpendicular to the columnar axis—that is why we chose the same resistivity scale ρ_M for both $\hat{\rho}_M$ and $\hat{\rho}_e$, while $\rho_I/\rho_M\to\infty$. The other parameters α_e, β_e, γ_e, λ_e, ν_M, H_M are all dimensionless and of order 1. The parameter H_M will be of special interest, since it denotes the Hall-to-transverse Ohmic resistivity of the M component. It can also be expressed in terms of the Hall mobility μ as $H_M=\mu|\mathbf{B}|$, or as $H_M=\omega_c\tau$ in the case of a free-electron-like conductor, where $\omega_c=e|\mathbf{B}|/(mc)$ is the cyclotron frequency of the charge carriers and τ is the conductivity relaxation time. We note that the subsequent results would remain unchanged even if $\hat{\rho}_I/\rho_I$ had a more complicated form, as long as $\rho_I/\rho_M\to\infty$. The difference between the volume fractions of the two components $\Delta p\equiv p_M-p_I = 2(p_M-1/2)>0$ also measures the distance from the percolation threshold for an uncorrelated random mixture, where the threshold is $p_c=1/2$.

The results of Eqs. (2.12), (2.11) now become $\alpha_e = 1/p_M$, $\beta_e=H_M/p_M$. We use these results, as well as Eq. (A24) for $\hat{\gamma}_{\mathrm{inc}}$ of a cylindrical inclusion, in the matrix self-consistency equation (3.8). Due to the three-dimensional isotropy of the constituent resistivity tensors, and the two-dimensional isotropy of the inclusion shapes, no averaging is required beyond that which is already implied by the volume fractions p_j appearing in that equation. The two equations, obtained, respectively, from the yy and zz components of that equation, are

$$0 = -p_I\lambda_e\left(\gamma_e+\frac{H_M^2}{p_M}\right)+\left[\lambda_e\left(\gamma_e+\frac{H_M^2}{p_M}\right)\right]^{1/2}$$
$$\times\left(\Delta p\,\gamma_e-1-\frac{p_I}{p_M}H_M^2\right)+p_M\gamma_e^2+(H_M^2-1)\gamma_e-\frac{H_M^2}{p_M}, \tag{4.3}$$

$$0 = p_I\left[\lambda_e\left(\gamma_e+\frac{H_M^2}{p_M}\right)\right]^{1/2}-p_M\lambda_e+\nu_M. \tag{4.4}$$

As mentioned earlier, the second equation is the same as the one that would follow from USEMA, while the first one is definitely different, and leads to different results. By eliminating γ_e from these equations, one arrives at a quartic equation for λ_e, which can be factorized, somewhat tediously, to yield

$$0 = (\lambda_e-\nu_M)(p_M\lambda_e-\nu_M)$$
$$\times\left[\Delta p\lambda_e^2-2\lambda_e\left(\nu_M p_M+\frac{p_I^2(1-\nu_M+H_M^2)}{2p_M}\right)+\nu_M^2\right]. \tag{4.5}$$

The physical solution for λ_e is one of the zeros of the quadratic polynomial factor in the square brackets of Eq. (4.5), namely,

$$\lambda_e = \frac{1}{\Delta p}\left\{ \nu_M p_M + \frac{p_I^2(1-\nu_M+H_M^2)}{2p_M} \right.$$
$$\left. + p_I\left[\nu_M(1+H_M^2) + \frac{p_I^2[(1-\nu_M)^2+H_M^4]}{4p_M^2} \right]^{1/2} \right\}.$$

(4.6)

That is the only solution that reduces to the correct form $\lambda_e = 1/\Delta p$ when $H_M = 0$, $\nu_M = 1$, and $\Delta p > 0$. From Eqs. (4.4) and (4.6) one also gets the following simple relation between γ_e and λ_e:

$$\gamma_e - \lambda_e = \frac{1-\nu_M}{p_M}.$$

(4.7)

For the special case where $\hat{\rho}_M$ is a free-electron resistivity tensor, i.e., $\nu_M = 1$, these results reduce to particularly simple forms:

$$\lambda_e = \gamma_e = \frac{1}{\Delta p}\left[p_M + \frac{p_I^2 H_M^2}{2p_M} + p_I\left(1+H_M^2+\frac{p_I^2 H_M^4}{4p_M^2}\right)^{1/2} \right]$$

$$\cong \begin{cases} \dfrac{1}{\Delta p}\left[1 + \dfrac{p_I H_M^2}{2p_M} + O(H_M^4)\right], & |H_M| \ll 1 \\[2ex] 1 + p_I|H_M| + O(p_I^2 H_M^2), & 1 \ll |H_M| \ll \dfrac{1}{p_I} \\[2ex] \dfrac{1}{\Delta p}\left[\dfrac{p_I^2 H_M^2}{p_M} + 2p_M + O\left(\dfrac{1}{p_I^2 H_M^2}\right)\right], & |H_M| \gg \dfrac{1}{p_I}. \end{cases}$$

(4.8)

The fact that the bulk effective longitudinal resistivity component $\rho_\parallel^{(e)} = \rho_M \lambda_e$ and the bulk effective in-plane transverse resistivity component $\widetilde{\rho}_\perp^{(e)} = \rho_M \gamma_e$ came out to be equal in this case is unexpected: The two in-plane directions are inequivalent, even when $\nu_M = 1$, and one might have therefore expected to find $\lambda_e \neq \gamma_e$ even then. For columnar arrays with a periodic microstructure this expectation is indeed borne out.[17,18] It is not clear whether the equality $\lambda_e = \gamma_e$ when $\nu_M = 1$ is a result of the approximations used to derive CUSEMA. In any case, it is clear that even when $\nu_M \neq 1$, λ_e and γ_e both tend to the same limit, which is proportional to H_M^2, when $|H_M| \gg 1/p_I$.

It is noteworthy that both resistivity components do not saturate with increasing $\mathbf{B}$, but continue to increase as $H_M^2 \propto \mathbf{B}^2$ at very large fields $|H_M| = |\mu \mathbf{B}| \gg 1/p_I$. This is consistent with the strong field behavior of magnetoresistance found earlier to occur in a composite where a *two-dimensional periodic array* of parallel, infinitely long, insulating columnar inclusions are embedded in an otherwise homogeneous conducting host.[18] In contrast with the disordered structures under consideration here, in those periodic microstructures both $\widetilde{\rho}_\perp^{(e)}$ and $\rho_\parallel^{(e)}$ oscillate strongly with changes

in the direction of $\mathbf{B}$ in the plane perpendicular to the columnar axis. However, it was also found that $\widetilde{\rho}_\perp^{(e)} \propto \mathbf{B}^2$ without any saturation whatever the direction of $\mathbf{B}$, and that $\rho_\parallel^{(e)}$ exhibits similar behavior for almost all directions of $\mathbf{B}$: $\rho_\parallel^{(e)}$ saturates only when $\mathbf{B}$ points in an in-plane direction where there exist inclusion-free parallel slabs that span the system from end to end.[18]

When the mixture is dilute in the insulating constituent, namely, $p_I \ll 1$, then for fields of low and intermediate strength, when $|H_M| \ll 1/p_I$, the changes in λ_e and γ_e (i.e., the *relative magnetoresistivities* $\rho_\parallel^{(e)}/\rho_M - 1 = \lambda_e - 1$ and $\widetilde{\rho}_\perp^{(e)}/\rho_M - 1 = \gamma_e - 1$) are proportional to H_M^2 when $|H_M| \ll 1$, and to $|H_M|$ when $1 \ll |H_M| \ll 1/p_I$. This behavior can be understood by recalling the changes produced by a *single isolated inclusion*: In that case, extra dissipation is caused by a cigar-shaped region of strong current distortion that extends from the inclusion along the two directions $\pm \mathbf{B}$. That region has a cross section that is roughly equal to that of the inclusion, and a length that is roughly equal to the inclusion size multiplied by $|H_M|$.[38,39] In a system with many inclusions, distributed randomly with a mean density that is low enough so that their volume fraction p_I satisfies $p_I \ll 1/|H_M|$, the region of strong distortion around any inclusion will usually not overlap with distortion regions produced by other inclusions. In that case, interactions between those distortions are negligible, and the induced magnetoresistance of the entire system will simply reflect the totality of extra dissipation produced by many isolated inclusions. Only at fields strong enough so that $p_I \gtrsim 1/|H_M|$ will those interactions become important, causing a gradual saturation of the in-plane current components J_y and J_z. In that case the columnar axis current component J_x will usually exhibit nonsaturating $J_x \propto H_M$ behavior, leading to H_M^2 behavior of the magnetoresistance, as shown in Sec. II.

We note that a microstructure similar to the disordered one under discussion here was already considered many years ago, namely, a system of parallel cylindrical inclusions, embedded in a free-electron host, in the presence of a magnetic field perpendicular to the columnar axis (see Figs. 1 and 2 of Ref. 24). But the inclusions were assumed to be open-orbit crystallites, and the discussion was based on a simpler Clausius-Mossotti– (or Maxwell Garnett–)type approximation. The fact, that a nonsaturating, $\mathbf{B}^2$ magnetoresistance will appear in a free-electron metal film with a random collection of perpendicular cylindrical holes, was not appreciated previously, and is shown here.

For the microstructure under consideration, it is also relatively easy to apply CMTA, by assuming that the composite inclusion also has a circular-cylinder shape and using $\hat{\gamma}_{\text{inc}}$ of Eq. (A25) in Eq. (3.4). In this case, for a conductor/insulator mixture, the exact relations of Sec. II are automatically satisfied. We thus get the following results for $\lambda_{e\,\text{CM}}$ and $\gamma_{e\,\text{CM}}$:

$$\lambda_{e\,\text{CM}} = \frac{\nu_M + p_I[\nu_M(1+H_M^2)]^{1/2}}{p_M},$$

(4.9)

$$\gamma_{e\,\text{CM}} = \lambda_{e\,\text{CM}} + \frac{1-\nu_M}{p_M} = \frac{1 + p_I[\nu_M(1+H_M^2)]^{1/2}}{p_M}.$$

(4.10)

These results can be compared with the results of CUSEMA, Eqs. (4.6), (4.7), or (4.8) for the case $\nu_M = 1$. The two approximations make similar predictions when p_I is small, but only for weak and intermediate fields, when $|H_M| \ll 1/p_I$. In the opposite case, when $|H_M| \gg 1/p_I$, they predict a drastically different behavior: CMTA continues to predict an asymptotic $\propto |H_M|$ behavior, whereas CUSEMA predicts an asymptotic $\propto H_M^2$ behavior. As explained above, the latter prediction is consistent with numerical calculations, as well as with exact results, on periodic microstructures,[10,17,18] and is due to interactions between the current distortion patterns produced by different inclusions. Thus, it seems as though CMTA does not take proper account of those interactions even for a dilute collection of inclusions $p_I \ll 1$. We note that, when $|H_M| \gg 1$, the cigar-shaped current distortion caused by an isolated inclusion is very different from the well known dipolar distortion that appears around an isolated spherical or cylindrical inclusion when $H_M = 0$.[39] Therefore, the fact that the CMTA takes into account the interactions between *dipolar distortions* is insufficient to account for the interactions when $|H_M| \gg 1$.

The results shown in Eq. (4.8) obviously exhibit divergent behavior for the magnetic-field-dependent parts of γ_e at the percolation threshold, where $\Delta p \to 0^+$. However, we do not expect the critical exponents obtained in this way to be accurate, as is usual in the case of effective-medium approximations of this kind.[40]

B. Disordered normal conductor/perfect conductor mixture

The effective-medium resistivity tensor $\hat{\rho}_e$ is again assumed to have the form of Eq. (4.1), and the normal conductor resistivity tensor is assumed to have the form of Eq. (4.2). The perfect conductor resistivity tensor has the form

$$\hat{\rho}_S = \rho_S \begin{pmatrix} 1 & -H_S & 0 \\ H_S & 1 & 0 \\ 0 & 0 & \nu_S \end{pmatrix}, \qquad (4.11)$$

where $\rho_S/\rho_M \to 0$. The subsequent results will not change even if $\hat{\rho}_S/\rho_S$ has a different form, as long as $\rho_S/\rho_M \to 0$. The volume fraction difference $\Delta p \equiv p_M - p_S = 2(p_M - 1/2)$ again measures the distance from the percolation threshold $p_c = 1/2$. We confine our discussion to the case $\Delta p > 0$, which means that the S component does not percolate, there-

fore we can continue to use a common absolute resistivity scale ρ_M for the effective medium as well as for the M component.

The exact results of Eqs. (2.12) and (2.11) now become $p_S \alpha_e = \rho_S/\rho_M$, $p_S \beta_e = [H_S + \gamma_e(H_S - H_M)/(1 + H_M^2)]\rho_S/\rho_M$. The two equations, obtained, respectively, from the yy and zz components of Eq. (3.8), are now

$$0 = (\gamma_e \lambda_e)^{1/2} \left(\frac{\gamma_e}{1 + H_M^2} - p_M \right) + p_S \gamma_e, \qquad (4.12)$$

$$0 = (\gamma_e \lambda_e)^{1/2} \left(\frac{\lambda_e}{\nu_M} - p_M \right) + p_S \lambda_e. \qquad (4.13)$$

In contrast with Eqs. (4.3) and (4.4), these are easily transformed into a quadratic equation for either of the two unknowns λ_e, γ_e. The equation thus obtained for γ_e is

$$0 = \left(\frac{\gamma_e}{1 + H_M^2} \right)^2 - 2 \frac{\gamma_e}{1 + H_M^2} \left[p_M + \frac{p_S^2(1 + H_M^2 - \nu_M)}{2 p_M \nu_M} \right] + \Delta p. \qquad (4.14)$$

The physical solution, i.e., the one that reduces to $\lambda_e = \gamma_e = \Delta p$ when $H_M = 0$ and $\nu_M = 1$, is

$$\frac{\gamma_e}{1 + H_M^2} = p_M + \frac{p_S^2(1 - \nu_M + H_M^2)}{2 p_M \nu_M}$$

$$- p_S \left[1 + \frac{1 - \nu_M + H_M^2}{\nu_M} + \frac{p_S^2(1 - \nu_M + H_M^2)^2}{4 p_M^2 \nu_M^2} \right]^{1/2}, \qquad (4.15)$$

$$\frac{1}{\lambda_e} = \frac{1}{\gamma_e} + \frac{1}{p_M} \left(\frac{1}{\nu_M} - \frac{1}{1 + H_M^2} \right). \qquad (4.16)$$

In the limit $p_S \to 0$ this leads to the correct result $\lambda_e = \nu_M$, but also to the incorrect result $\gamma_e = 1 + H_M^2$, instead of $\gamma_e = 1$. This reflects the fact that $p_S \to 0$ is a *singular limit*: Although $E_x = 0$ for any $p_S \neq 0$, when $p_S = 0$ that field component, though still uniform, ceases to vanish. Consequently, α_e and β_e also cease to vanish. Therefore some of the results obtained in this subsection are expected to be invalidated when $p_S = 0$. In the limits $|H_M| \ll 1$ and $|H_M| \gg 1$, Eq. (4.15) becomes

$$\frac{\gamma_e}{1 + H_M^2} \cong \begin{cases} \Delta p + \dfrac{p_S}{2 p_M \nu_M} \{2 p_M \nu_M + p_S(1 - \nu_M) - [4 p_M^2 \nu_M + p_S^2(1 - \nu_M)^2]^{1/2}\} \\ \quad + \dfrac{p_S H_M^2}{2 p_M \nu_M} \left[p_S - \dfrac{\nu_M(p_M^2 + \Delta p) + p_S^2}{[4 p_M^2 \nu_M + p_S^2(1 - \nu_M)^2]^{1/2}} \right], & |H_M| \ll 1 \\[4mm] \Delta p - \dfrac{p_S|H_M|}{\nu_M^{1/2}}, & 1 \ll |H_M| \ll \dfrac{1}{p_S} \\[4mm] \dfrac{\nu_M p_M \Delta p}{p_S^2 H_M^2}, & |H_M| \gg \dfrac{1}{p_S}. \end{cases} \qquad (4.17)$$

When $\nu_M = 1$, these equations simplify to

$$\frac{\gamma_e}{1+H_M^2} = p_M + \frac{p_S^2 H_M^2}{2p_M} - p_S \left(1 + H_M^2 + \frac{p_S^2 H_M^4}{4p_M^2} \right)^{1/2},$$
(4.18)

$$\frac{1}{\lambda_e} = \frac{1}{\gamma_e} + \frac{H_M^2/p_M}{1+H_M^2},$$
(4.19)

$$\gamma_e \cong \begin{cases} \Delta p \left[1 + \dfrac{H_M^2(p_M + \Delta p)}{2p_M} \right], & |H_M| \ll \dfrac{1}{p_S} \\[2ex] \dfrac{p_M \Delta p}{p_S^2}, & |H_M| \gg \dfrac{1}{p_S}, \end{cases}$$
(4.20)

$$\lambda_e \cong \begin{cases} \Delta p \left[1 + \dfrac{p_S H_M^2}{2p_M} \right], & |H_M| \ll 1 \\[2ex] \dfrac{1}{p_M}, & |H_M| \gg 1. \end{cases}$$
(4.21)

These results can be compared with some results obtained many years ago for *three-dimensional* normal conductor/perfect conductor random mixtures using USEMA:[41] There it was found that $\widetilde{\rho}_\perp^{(e)}$ saturates at strong fields, but a linear increase with H_M was found to appear at intermediate fields. We do not find such an intermediate regime, either for $\widetilde{\rho}_\perp^{(e)} = \rho_M \gamma_e$ or for $\rho_\parallel^{(e)} = \rho_M \lambda_e$. The fact that both γ_e and λ_e saturate at large fields $|H_M| \gg 1$ is again consistent with previous results for columnar composites, where a periodic array of perfectly conducting inclusions are embedded in a normal conductor host:[18] In that case, $\rho_\parallel^{(e)}$ was found to saturate whatever the direction of **B** in the perpendicular plane, while $\widetilde{\rho}_\perp^{(e)}$ was found to saturate for almost all directions of **B**, except for those few where there are system spanning, inclusion-free, parallel slabs.

Equations (4.15) and (4.16) also show that γ_e and λ_e tend to 0, in the same fashion, as p_M approaches the percolation threshold $p_c = 1/2$ from above.

In this case, the CMTA again satisfies the exact relations of Sec. II automatically. The results for λ_e and γ_e are

$$\lambda_e = \frac{p_M \nu_M (1+H_M^2)}{1+H_M^2 + p_S[\nu_M(1+H_M^2)]^{1/2}},$$
(4.22)

$$\gamma_e = \frac{p_M \nu_M (1+H_M^2)}{\nu_M + p_S[\nu_M(1+H_M^2)]^{1/2}}.$$
(4.23)

These results satisfy Eq. (4.16), and they reduce to the correct form $\gamma_e = \lambda_e = p_M/(1+p_S)$ when $H_M = 0$ and $\nu_M = 1$. When $p_S \to 0$, λ_e reduces to the correct result ν_M, while γ_e again yields the wrong result $1+H_M^2$ instead of 1. When $|H_M| \gg 1$, λ_e saturates at $p_M \nu_M$, but when $|H_M| \gg 1/p_S$, then $\gamma_e \cong p_M \nu_M^{1/2} |H_M|/p_S$, i.e., it continues to increase without any saturation. From our previous discussion of CUSEMA, this behavior of γ_e is qualitatively wrong. These CMTA behaviors of λ_e and γ_e are similar to what was found many

years ago in three-dimensional normal conductor/perfect conductor mixtures using the dilute approximation.[42]

V. SUMMARY AND DISCUSSION

We have shown that there exist some exact relations among elements of the bulk effective resistivity tensor of a composite medium with a columnar microstructure. Those relations are usually violated by naive extensions to such structures of the Bruggeman self-consistent effective-medium approximation. In particular, this occurs when a magnetic field is present that is perpendicular to the columnar axis: It results from the coupling between electric field and current components along the columnar axis and similar components that are perpendicular to that axis. We therefore proposed a different extension of the Bruggeman approximation, namely the ''columnar unambiguous self-consistent effective-medium approximation,'' which incorporates those exact relations. We then applied CUSEMA to disordered conductor/insulator mixtures and to normal conductor/perfect conductor mixtures, where all constituents were assumed to exhibit isotropic electrical response, and where a magnetic field is present that is perpendicular to the columnar axis.

In the conductor/insulator mixtures we found that both the longitudinal and the in-plane transverse magnetoresistivities, $\rho_\parallel^{(e)}$ and $\widetilde{\rho}_\perp^{(e)}$ increase as $\mathbf{B}^2$ *without any saturation* for sufficiently strong fields. This remains true even when the mixture is very dilute in the insulating component: The unsaturated $\mathbf{B}^2$ behavior appears whenever $|\mu\mathbf{B}| \gg 1/p_I$. By contrast, in the normal conductor/perfect conductor mixtures we found that both $\rho_\parallel^{(e)}$ and $\widetilde{\rho}_\perp^{(e)}$ approach constant asymptotic values at comparably large fields, i.e., when $|\mu\mathbf{B}| \gg 1/p_S$. The CMTA does not reproduce the correct behavior at strong fields for either type of mixture: In the case of conductor/insulator mixtures it has both $\rho_\parallel^{(e)}$ and $\widetilde{\rho}_\perp^{(e)}$ increasing only as $|\mathbf{B}|$ even when $\mathbf{B}$ is very large. This is due to inadequate treatment of interactions between current distortion effects of different inclusions in that approximation. In the case of normal conductor/perfect conductor mixtures it has $\rho_\parallel^{(e)}$ saturating but $\widetilde{\rho}_\perp^{(e)}$ increasing as $|\mathbf{B}|$ for large $\mathbf{B}$, when $|\mu\mathbf{B}| \gg 1/p_S$. We conclude that for strong fields, when $|\mu\mathbf{B}| \gtrsim 1/p_I$ or $|\mu\mathbf{B}| \gtrsim 1/p_S$, CMTA is not a good approximation even for a very dilute collection of inclusions. A large discrepancy between the predictions of CMTA and those of a Bruggeman-type self-consistent effective-medium approximation or USEMA, for magnetotransport in certain types of three-dimensional composites, was already found many years ago by Stroud and Pan.[24] The more powerful tools that we were able to deploy for the study of columnar microstructures, along with the explicit algebraic expressions that we obtained, enabled us to better understand the reasons for such discrepancies in that case. Work is in progress to apply some of this understanding also to magnetotransport in three-dimensional disordered microstructures.

In both types of random mixtures that we considered (i.e., conductor/insulator mixtures and normal conductor/perfect conductor mixtures), the magnetoresistivity components exhibit critical behavior as the two-dimensional percolation threshold of the normal conducting constituent is approached

from above. It will be interesting to study this behavior using methods that are more reliable than CUSEMA, which is expected to fail near that threshold.

The results obtained in this work are applicable to thin conducting films with perpendicular holes, and also to thin semiconducting films with perpendicular metallic or superconducting inclusions. The only requirement is that the film thickness l and the inclusion radii a satisfy $a/l \ll |H_M| = |\mu \mathbf{B}|$. Work is currently in progress to extend these results to two-component mixtures where both constituents have finite resistivity tensors.

ACKNOWLEDGMENTS

APPENDIX: ISOLATED ELLIPSOIDAL INCLUSION

We start by recalling that the local electric potential $\phi(\mathbf{r})$ in an inhomogeneous conductor can be found by solving the following boundary-value problem:

$$\nabla \cdot [\hat{\sigma}(\mathbf{r}) \cdot \nabla \phi(\mathbf{r})] = 0 \quad \text{in the entire volume } V, \quad \text{(A1)}$$

$$\phi(\mathbf{r}) = -(\mathbf{E}_0 \cdot \mathbf{r}) \quad \text{at the external surface } \partial V, \quad \text{(A2)}$$

where $\mathbf{E}_0$ is the volume-averaged electric field and $\hat{\sigma}(\mathbf{r})$ is the local conductivity tensor, which is nonsymmetric in the presence of a magnetic field $\mathbf{B}$. We can express $\hat{\sigma}(\mathbf{r})$ in terms of the constituent conductivity tensors $\hat{\sigma}_i$ and the characteristic (or indicator) functions $\theta_i(\mathbf{r})$ [$\theta_i(\mathbf{r}) = 1$ if $\hat{\sigma}(\mathbf{r}) = \hat{\sigma}_i$, and $\hat{\sigma}(\mathbf{r}) = 0$ otherwise]. In the case of a two-constituent composite medium we can thus write,

$$\hat{\sigma}(\mathbf{r}) = \hat{\sigma}_1 \theta_1(\mathbf{r}) + \hat{\sigma}_2 \theta_2(\mathbf{r}) = \hat{\sigma}_2 - \delta\hat{\sigma} \theta_1(\mathbf{r}), \quad \text{(A3)}$$

$$\delta\hat{\sigma} \equiv \hat{\sigma}_2 - \hat{\sigma}_1. \quad \text{(A4)}$$

Using this, the differential Eq. (A1) becomes

$$\nabla \cdot \hat{\sigma}_2 \cdot \nabla \phi = \nabla \cdot \delta\hat{\sigma} \theta_1 \nabla \phi. \quad \text{(A5)}$$

The left-hand side of this equation is simple enough (i.e., a second-order elliptic differential operator with constant coefficients) that it is useful to define its Green's function $G(\mathbf{r}, \mathbf{r}' | \hat{\sigma}_2)$:

$$\nabla \cdot \hat{\sigma}_2 \cdot \nabla G = -\delta^3(\mathbf{r} - \mathbf{r}') \quad \text{for } \mathbf{r} \in V, \quad \text{(A6)}$$

$$G = 0 \quad \text{for } \mathbf{r} \in \partial V. \quad \text{(A7)}$$

Note that G depends only on the symmetric part of the tensor $\hat{\sigma}_2$. Using G, we can transform the boundary-value problem of Eqs. (A1) and (A2) to an integrodifferential equation for $\phi(\mathbf{r})$,

$$\phi = -\mathbf{E}_0 \cdot \mathbf{r} - \int dV' G(\mathbf{r}, \mathbf{r}' | \hat{\sigma}_2) \nabla' \cdot (\theta_1' \delta\hat{\sigma} \cdot \nabla' \phi') \quad \text{(A8)}$$

$$= -\mathbf{E}_0 \cdot \mathbf{r} + \int dV' \theta_1' (\nabla' G \cdot \delta\hat{\sigma} \cdot \nabla' \phi'), \quad \text{(A9)}$$

or

$$\mathbf{E}(\mathbf{r}) = -\nabla \phi = \mathbf{E}_0 + \int dV' \theta_1' \nabla \nabla' G \cdot \delta\hat{\sigma} \cdot \mathbf{E}'. \quad \text{(A10)}$$

Here we used the abbreviated notation ϕ' for $\phi(\mathbf{r}')$, etc. When V is infinite, $G(\mathbf{r}, \mathbf{r}' | \hat{\sigma})$ depends only on the separation vector $\mathbf{r} - \mathbf{r}'$. The Fourier transform of G then has the simple form

$$\int dV e^{-\mathbf{k} \cdot (\mathbf{r} - \mathbf{r}')} G(\mathbf{r}, \mathbf{r}' | \hat{\sigma}) = \frac{1}{(\mathbf{k} \cdot \hat{\sigma} \cdot \mathbf{k})}. \quad \text{(A11)}$$

G itself also has a fairly simple form, if the coordinate axes are chosen to lie along the principal axes of the symmetric part of the tensor $\hat{\sigma}$

$$G(\mathbf{r}, \mathbf{r}' | \hat{\sigma}) = \frac{1}{4\pi(\sigma_{xx}\sigma_{yy}\sigma_{zz})^{1/2}}$$
$$\times \left(\frac{(x-x')^2}{\sigma_{xx}} + \frac{(y-y')^2}{\sigma_{yy}} + \frac{(z-z')^2}{\sigma_{zz}} \right)^{-1/2}. \quad \text{(A12)}$$

If we consider the case of a single inclusion $\hat{\sigma}_1$, of ellipsoidal shape, embedded in a uniform host medium $\hat{\sigma}_2$, then we can solve Eq. (A9) in a fairly explicit manner. We can also show that the electric field inside the inclusion is uniform, no matter how complicated the tensors $\hat{\sigma}_1$, $\hat{\sigma}_2$.

In order to show this, we transform to a new system of Cartesian coordinates: First we align the coordinate axes along the principal axes of the symmetric part of $\hat{\sigma}_2$. Then we rescale the coordinate axes as follows

$$\xi_1 \equiv \frac{x}{\sqrt{\sigma_{xx}^{(2)}}}, \quad \xi_2 \equiv \frac{y}{\sqrt{\sigma_{yy}^{(2)}}}, \quad \xi_3 \equiv \frac{z}{\sqrt{\sigma_{zz}^{(2)}}}. \quad \text{(A13)}$$

This changes the shape of the inclusion, but it still remains an ellipsoid. It also greatly simplifies the form of G, which becomes proportional to the Coulomb potential $1/|\boldsymbol{\xi} - \boldsymbol{\xi}'|$. Eq. (A10) becomes

$$E_\alpha(\boldsymbol{\xi}) = E_{0\alpha} + \sum_{\beta,\gamma} \frac{1}{(\sigma_{\alpha\alpha}^{(2)}\sigma_{\beta\beta}^{(2)})^{1/2}}$$

$$\times \int_{V_{\rm ell}} d^3\xi' \frac{\partial}{\partial\xi_\alpha} \frac{\partial}{\partial\xi'_\beta} \frac{1}{4\pi|\boldsymbol{\xi}-\boldsymbol{\xi}'|} \delta\sigma_{\beta\gamma} E_\gamma(\boldsymbol{\xi}'),$$

(A14)

where the integration volume $V_{\rm ell}$ in $\boldsymbol{\xi}$ space is the volume of the *transformed* ellipsoidal inclusion.

We now recall the fact that, if both components are isotropic conductors and $\mathbf{B}=0$, (i.e., $\hat{\sigma}_1$, $\hat{\sigma}_2$ are scalar tensors) and if $\mathbf{E}_0$ lies along a principal axis α of an isolated ellipsoidal inclusion, then the electric field inside that inclusion is uniform and points in the same direction, and its magnitude is given by (see, e.g., Ref. 32)

$$\frac{E_{0\alpha}\sigma_2}{\sigma_1 n_\alpha + \sigma_2(1-n_\alpha)}.$$

(A15)

Here n_α is the appropriate depolarization factor. Using this result in Eqs. (A10) or (A14), we easily get

$$n_\alpha \delta_{\alpha\beta} = \int_{V_{\rm ell}} dV' \boldsymbol{\nabla}_\alpha \boldsymbol{\nabla}'_\beta \frac{1}{4\pi|\mathbf{r}-\mathbf{r}'|} \quad \text{for} \quad \mathbf{r} \in V_{\rm ell},$$

(A16)

which is valid if the coordinate axes are the principal axes of the inclusion. For other choices of coordinate axes this generalizes to

$$n_{\alpha\beta} = \int_{V_{\rm ell}} dV' \boldsymbol{\nabla}_\alpha \boldsymbol{\nabla}'_\beta \frac{1}{4\pi|\mathbf{r}-\mathbf{r}'|} \quad \text{for} \quad \mathbf{r} \in V_{\rm ell},$$

(A17)

where $n_{\alpha\beta}$ are Cartesian components of the depolarization tensor. An important conclusion from this discussion is that the last integral is independent of $\mathbf{r}$ inside $V_{\rm ell}$. It is important to remember that this tensor depends on the shape of the *transformed inclusion*. However, that shape depends upon the conductivity tensor $\hat{\sigma}_2$ of the host medium, therefore $n_{\alpha\beta}$ will also depend on $\hat{\sigma}_2$.

In order to test the proposition that $\mathbf{E}(\mathbf{r})$ is a constant $\mathbf{E}_{\rm int}$ inside $V_{\rm ell}$ in the *general case*, we substitute that ansatz in Eq. (A14). Using Eq. (A17), we thus get the following set of three linear algebraic equations for the components of $\mathbf{E}_{\rm int}$:

$$E_{{\rm int}\alpha} = E_{0\alpha} + \sum_{\beta,\gamma} \frac{n_{\alpha\beta}\delta\sigma_{\beta\gamma}}{(\sigma_{\alpha\alpha}^{(2)}\sigma_{\beta\beta}^{(2)})^{1/2}} E_{{\rm int}\gamma}.$$

(A18)

These equations usually have a unique solution, in which case the above-mentioned proposition is verified. When the determinant of these equations vanishes, it means that the

system has a so-called *quasistatic resonance*.[14] This is an interesting phenomenon in its own right, but it can only occur at nonzero frequencies.

We note that the solution for $\mathbf{E}_{\rm int}$ depends upon $\hat{\sigma}_2$ also through $n_{\alpha\beta}$, since the precise shape of the transformed ellipsoid, of volume $V_{\rm ell}$, depends on $\hat{\sigma}_2$. The final dependence of $\mathbf{E}_{\rm int}$ on the conductivity or resistivity tensors and on the actual shape of the original inclusion is thus, in general, quite complicated.

Obviously, Eqs. (A18) show that we can write

$$\mathbf{E}_{\rm int} = \hat{\gamma}_{\rm inc} \cdot \mathbf{E}_0,$$

(A19)

where the elements of the inverse matrix $1/\hat{\gamma}_{\rm inc}$ are given by

$$\left(\frac{1}{\hat{\gamma}_{\rm inc}}\right)_{\alpha\gamma} = \delta_{\alpha\gamma} - \sum_\beta \frac{n_{\alpha\beta}\delta\sigma_{\beta\gamma}}{(\sigma_{\alpha\alpha}^{(2)}\sigma_{\beta\beta}^{(2)})^{1/2}}.$$

(A20)

As an example, which is relevant for Sec. IV, we consider an inclusion that has a fully isotropic electrical response and is shaped as an infinitely long circular cylinder along the x axis. The host has an electrical response that may be anisotropic, but x is one of its principal axes. Along one of its other principal axes a uniform magnetic field $\mathbf{B}$ is applied—that is taken to be the z axis. Consequently, the resistivity tensors must have the following forms:

$$\hat{\rho}_{\rm host} = \rho_0 \begin{pmatrix} \alpha & -\beta & 0 \\ \beta & \gamma & 0 \\ 0 & 0 & \lambda \end{pmatrix},$$

(A21)

$$\hat{\rho}_{\rm inc} = \rho_1 \begin{pmatrix} 1 & -H & 0 \\ H & 1 & 0 \\ 0 & 0 & \nu \end{pmatrix}.$$

(A22)

The rescaling transformation of Eqs. (A13) changes the infinitely long circular cylinder into an infinitely long elliptic cylinder, with major axes along x, y, and z. The depolarization factor along each major axis of such a cylinder is inversely proportional to the length of that axis (see, e.g., Ref. 32), therefore those factors are given by

$$n_y = \frac{(\sigma_{{\rm host}\,yy})^{1/2}}{(\sigma_{{\rm host}\,zz})^{1/2} + (\sigma_{{\rm host}\,yy})^{1/2}} = \frac{1}{\left(\dfrac{\gamma+\beta^2/\alpha}{\lambda}\right)^{1/2}+1},$$

$$n_z = 1 - n_y, \quad n_x = 0.$$

(A23)

From these it is a straightforward procedure to calculate the matrix $\hat{\gamma}_{\rm inc}$, which comes out to be

$$\hat{\gamma}_{\text{inc}} = \begin{pmatrix} 1 & 0 & 0 \\ \dfrac{-\dfrac{\beta}{\alpha} + \dfrac{\rho_0}{\rho_1}(\gamma+\beta^2/\alpha)\dfrac{H}{1+H^2}}{\left(\dfrac{\gamma+\beta^2/\alpha}{\lambda}\right)^{1/2} + (\gamma+\beta^2/\alpha)\dfrac{\rho_0/\rho_1}{1+H^2}} & \dfrac{1+\left(\dfrac{\gamma+\beta^2/\alpha}{\lambda}\right)^{1/2}}{\left(\dfrac{\gamma+\beta^2/\alpha}{\lambda}\right)^{1/2} + (\gamma+\beta^2/\alpha)\dfrac{\rho_0/\rho_1}{1+H^2}} & 0 \\ 0 & 0 & \dfrac{1+\left(\dfrac{\gamma+\beta^2/\alpha}{\lambda}\right)^{1/2}}{1+\dfrac{\rho_0}{\rho_1}\dfrac{\lambda}{\nu}\left(\dfrac{\gamma+\beta^2/\alpha}{\lambda}\right)^{1/2}} \end{pmatrix}. \tag{A24}$$

This is used in Sec. IV to derive the columnar unambiguous self-consistent effective-medium approximation for columnar composites.

If we switch the roles of host and inclusion, so that Eqs. (A21) and (A22) now represent $\hat{\rho}_{\text{inc}}$ and $\hat{\rho}_{\text{host}}$, respectively, then we similarly find

$$\hat{\gamma}_{\text{inc}} = \begin{pmatrix} 1 & 0 & 0 \\ \dfrac{-\nu H + \dfrac{\beta/\alpha}{\gamma+\beta^2/\alpha}\nu(1+H^2)\dfrac{\rho_1}{\rho_0}}{[\nu(1+H^2)]^{1/2} + \dfrac{\nu(1+H^2)}{\gamma+\beta^2/\alpha}\dfrac{\rho_1}{\rho_0}} & \dfrac{\nu + [\nu(1+H^2)]^{1/2}}{[\nu(1+H^2)]^{1/2} + \dfrac{\nu(1+H^2)}{\gamma+\beta^2/\alpha}\dfrac{\rho_1}{\rho_0}} & 0 \\ 0 & 0 & \dfrac{\nu + [\nu(1+H^2)]^{1/2}}{\nu + \dfrac{\nu}{\lambda}[\nu(1+H^2)]^{1/2}\dfrac{\rho_1}{\rho_0}} \end{pmatrix}. \tag{A25}$$

This is needed in order to derive the Clausius-Mossotti–type approximation for columnar composites—Eqs. (4.9), (4.10), (4.22), and (4.23).

[1] R. Juretschke, R. Landauer, and J. A. Swanson, J. Appl. Phys. **27**, 838 (1956).

[2] D. J. Bergman, Y. Kantor, D. Stroud, and I. Webman, Phys. Rev. Lett. **50**, 1512 (1983).

[3] D. Stroud and D. J. Bergman, Phys. Rev. B **30**, 447 (1984).

[4] D. J. Bergman and D. Stroud, Phys. Rev. B **32**, 6097 (1985).

[5] D. J. Berman, E. Duering, and M. Murat, J. Stat. Phys. **58**, 1 (1990).

[6] U. Dai, A. Palevski, and G. Deutscher, Phys. Rev. B **36**, 790 (1987).

[7] D. J. Bergman, Philos. Mag. B **56**, 983 (1987).

[8] A. K. Sarychev, D. J. Bergman, and Y. M. Strelniker, Europhys. Lett. **21**, 851 (1993).

[9] A. K. Sarychev, D. J. Bergman, and Y. M. Strelniker, Phys. Rev. B **48**, 3145 (1993).

[10] D. J. Bergman and Y. M. Strelniker, Phys. Rev. B **49**, 16 256 (1994).

[11] Y. M. Strelniker and D. J. Bergman, Phys. Rev. B **50**, 14 001 (1994).

[12] Y. M. Strelniker and D. J. Bergman, Phys. Rev. B **53**, 11 051 (1996).

[13] M. Barthelemy and D. J. Bergman, Phys. Rev. B **58**, 12 770 (1998).

[14] D. J. Bergman and D. Stroud, Solid State Phys. **46**, 147 (1992).

[15] M. Tornow, D. Weiss, K. v. Klitzing, K. Eberl, D. J. Bergman, and Y. M. Strelniker, Phys. Rev. Lett. **77**, 147 (1996).

[16] D. J. Bergman and Y. M. Strelniker, Superlattices Microstruct. **23**, 547 (1998).

[17] D. J. Bergman and Y. M. Strelniker, Phys. Rev. Lett. **80**, 3356 (1998).

[18] D. J. Bergman and Y. M. Strelniker, Phys. Rev. B **59**, 2180 (1999).

[19] D. J. Bergman and Y. M. Strelniker, Europhys. Lett. **45**, 605 (1999).

[20] D. A. G. Bruggeman, Ann. Phys. (Leipzig) **24**, 636 (1935).

[21] H. Stachowiak, Physica (Amsterdam) **45**, 481 (1970).

[22] M. H. Cohen and J. Jortner, Phys. Rev. Lett. **30**, 696 (1973).

[23] D. Stroud, Phys. Rev. B **12**, 3368 (1975).

[24] D. Stroud and F. P. Pan, Phys. Rev. B **20**, 455 (1979).

[25] R. Landauer, J. Appl. Phys. **23**, 779 (1952).

[26] P. Soven, Phys. Rev. **156**, 809 (1967).

[27] H. Ehrenreich and L. M. Schwartz, Solid State Phys. **31**, 149 (1976).

[28] J. S. Faulkner, Prog. Mater. Sci. **27**, 1 (1982).

[29] D. J. Bergman, Phys. Rev. B **39**, 4598 (1989).

[30] D. J. Bergman, in *Composite Media and Homogenization Theory*, edited by G. Dal Maso and G. F. Dell'Antonio (Birkhäuser, Berlin, 1991), pp. 67–79.

[31] L. Sali and D. J. Bergman, J. Stat. Phys. **86**, 455 (1997).

[32] L. D. Landau, E. M. Lifshitz, and L. P. Pitaevskiĭ, *Electrodynamics of Continuous Media*, 2nd ed. (Pergamon, New York, 1984).

[33] J. P. Straley, J. Phys. C **13**, 4335 (1980).

[34] J. P. Straley, in *Percolation Structures and Processes*, edited by G. Deutscher, R. Zallen, and A. Adler [J. Phys. C **13**, L773 (1980)].

[35] D. J. Bergman, Ann. Isr. Phys. Soc. **5**, 297 (1983).

[36] A. Palevski, M. L. Rappaport, A. Kapitulnik, A. Fried, and G. Deutscher, J. Phys. (France) Lett. **45**, L367 (1984).

[37] D. J. Bergman and Y. M. Strelniker, Phys. Rev. B **51**, 13 845 (1995).

[38] C. Herring, J. Appl. Phys. **31**, 1939 (1960).

[39] J. B. Sampsell and J. C. Garland, Phys. Rev. B **13**, 583 (1976).

[40] A. Aharony and D. Stauffer, *Introduction to Percolation Theory*, 2nd ed. (Taylor & Francis, London, 1992).

[41] D. Stroud, Phys. Rev. Lett. **44**, 1708 (1980).

[42] D. Stroud and F. P. Pan, Phys. Rev. B **13**, 1434 (1976).